

## FLOODED COUNTERCURRENT TWO-PHASE FLOW IN HORIZONTAL TUBES AND CHANNELS

G. C. GARDNER

Central Electricity Research Laboratories, Leatherhead, Surrey, England

(Received 28 January 1982; in revised form 5 December 1982)

**Abstract**—A criterion for flooding in the countercurrent flow of two fluids in horizontal tubes and channels is developed. It exhibits a dependence upon the density ratio of the fluids beyond that present in the criterion of Wallis (1969). Experiments were carried out with air and water in a horizontal tube at atmospheric pressure and these, together with others reported in the literature, are shown to be in fair agreement with the prediction of the criterion, though it is emphasised that more experimental work is desirable.

Work reported in the literature with miscible fluids with a density ratio close to unity confirms the extra dependence upon the density ratio.

### I. INTRODUCTION

One aspects of the discharge of a fluid from a vessel along a horizontal pipe with counterflow of gas is recognised by all who have poured themselves a drink from a bottle. If the bottle is tipped too rapidly to the horizontal position, the inflow of air, which makes up for the volume of the discharged beverage, restricts the discharge by an intermittent process that is sometimes called "glugging". More generally, the problem is that of determining the rate of fluid discharge against a counterflow of a lighter fluid at a given rate, which may be different, on a volumetric basis, from that of the denser fluid.

Until recently the problem has only received slight attention, presumably because such counterflow is not usually an intention in the design of apparatus or plant. It most often arises when equipment is operating under fault conditions but the prediction of the exchange flowrates may then be of critical importance. The two cases within the writer's experience both occur during hypothetical accidents to nuclear power plant.

In magnox reactors, carbon dioxide under pressure is circulated to cool the reactor and to transfer the heat to water in a steam generator. Carbon dioxide will be rapidly discharged if a horizontal circulating pipe is accidentally ruptured but, once the pressure inside the reactor system has reduced to near atmospheric pressure, air, with a density less than that of the carbon dioxide, will flow into the reactor against a counterflow of carbon dioxide. Experimental work on this subject has been carried out by Leach & Thompson (1975), Mercer & Thompson (1975) and Witherington (1978), using water and brine as fluids as well as carbon dioxide and air, and was restricted to equal volumetric flowrates of the two fluids, as in the case of pouring a drink from a bottle. Otherwise it is noted that the ratio of the densities of the two fluids did not exceed 1.2 and the fluids were miscible, so that surface tension was not a parameter. It was not mentioned by the above workers that the phenomenon of glugging occurred and there was no suggestion that the flows were erratic.

In pressurized water reactors, primary water under pressure is circulated through the reactor to remove heat, which is passed to secondary water in an evaporator. If the primary water circuit is breached so that water discharges to atmosphere, steam will form within the circuit due to depressurization and countercurrent flow of steam and water can occur. Of particular importance is the horizontal pipe or "hot leg" connecting the reactor to the bottom of the steam generator. If the breach does not occur in the pipe, water from the primary side of the evaporator may, with advantage, drain back to the reactor against a steam flow. In this case, the volumetric flowrates of the two phases will not, in general, be equal.

Richter *et al.* (1978) carried out experiments in a simulation of the pressurised water reactor's hot leg, as illustrated in figure 1. The pipe bore was 203 mm and they employed air

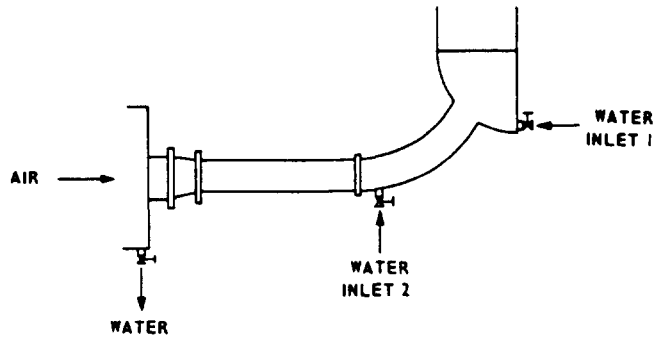


Figure 1. Diagram of apparatus of Richter *et al.* (1978).

and water as fluids. Attention was confined to the higher possible air flowrates and, consequently, to the lower possible water flowrates.

Krolewski (1980) carried out similar work with a 51 mm bore pipe with water inlets and outlets as illustrated in figure 2. She covered a wide range of flowrates of both phases and determined the air flowrate which just started to hold water back as the air flowrate increased and just started to release water at a given flowrate as the air flowrate was decreased. A strong hysteresis was found for the higher water flowrates in the pipe configurations *C* and *E*. On the basis of this work, a substantial hysteresis would not be expected for the flowrates employed by Richter *et al.* (1978).

This paper presents further air-water experimental results obtained with the system illustrated in figure 3 and compares them with a theory of steady state countercurrent flooded flow. The adjective "flooded" is employed in the sense that the air flow restricts that of the water. The results of the theory differ from that of Wallis (1969) not only in magnitude but, also, because an extra influence of the density ratio of the two fluids is exhibited.

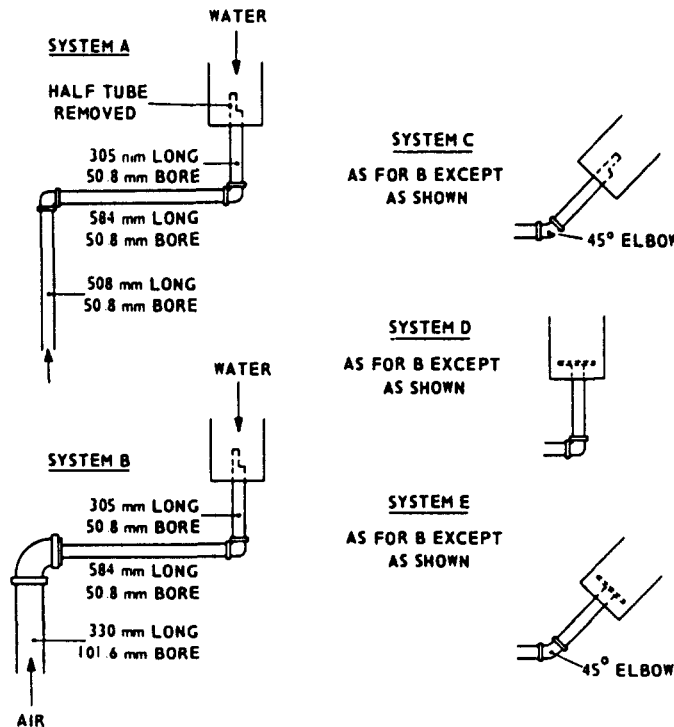


Figure 2. Diagram of the apparatus of Krolewski (1980).

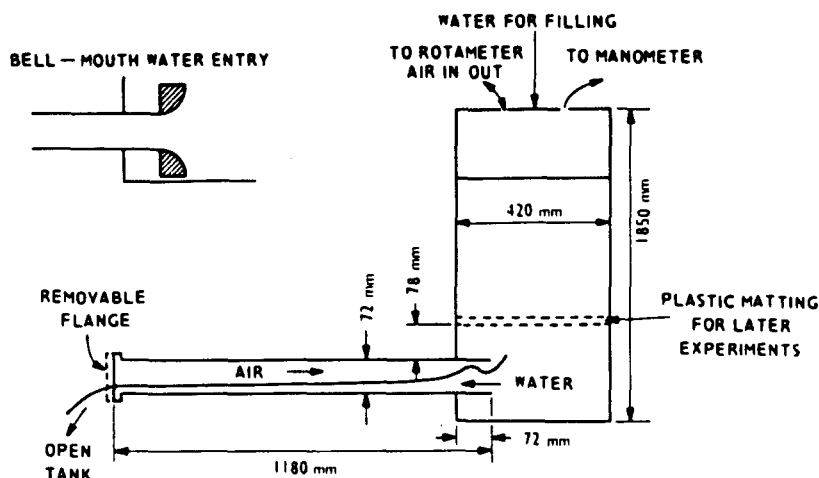


Figure 3. Diagram of apparatus for present experiments.

## 2. THE EXPERIMENTAL AND VISUAL OBSERVATIONS

Experiments were carried out with the apparatus illustrated in figure 3 and with air and water at atmospheric pressure as the fluids. The water chamber was constructed of 13 mm thick perspex supported by angle iron and was 1850 mm tall with a  $420 \times 420$  mm plan cross-section. A horizontal 72 mm bore, 1180 mm long perspex tube was set in and projected 72 mm through the vertical wall of the chamber with its centreline 140 mm above the chamber's base. The end of the tube far from the chamber was sealed with an easily removed blank flange so that the chamber could be filled with water without any discharge.

The top of the water chamber was sealed, except for connections to a water supply, to a water-in-glass manometer and to an air rotameter. Air could be drawn out of the top of the water chamber by a suction system when necessary.

The experiment started with the water chamber nearly full of water. The blank flange on the end of the discharge pipe was rapidly removed and the flow of air in or out of the top of the water chamber was set and controlled manually at a desired value. The manometer was read at 10 s intervals until the water level fell to about 100 mm above the top of the discharge tube.

The manometer reading was plotted vs time and a straight line was drawn through the data points. The slope of the line allowed the rate of water discharge to be calculated. Although the manometer water level fluctuated substantially, the data points formed a very satisfactory straight line and a regression analysis confirmed that the accuracy of the calculated water rate was within a few percent.

The air flowrate was the water flowrate plus the air flowrate out of the chamber through the rotameter. Appropriate corrections, which were based upon the pressure read by the manometer, had to be made to the rotameter reading to convert the flowrate to air at atmospheric pressure in the discharge tube. It is noted that the rotameter reading and the water discharge rate were essentially constant so that the calculated air flowrate through the discharge varied through the experiment. This accounts for the magnitude of the error bars which will be given on the graphs of results.

Two forms of water entry to the discharge tube were employed. One was simply a sharp-edged pipe entry and the other was the bell-mouth entry shown in figure 3.

Vigorous chugging was observed with both forms of water entry for all flows in which air was allowed to be drawn into the top of the water chamber to reduce the amount of air flowing in the discharge tube. A limited amount of air would rapidly pass into the water chamber and then the water entry end of the tube would be suddenly filled with water to a length of up to 300 mm. A long air bubble, with a characteristic depth of about half the tube diameter, would

then flow through the plug of water until it reached the end of the tube in the water chamber. The cycle would then be repeated. Presumably the release of air into the water chamber rapidly increases the pressure in the chamber so that a plug of water was ejected. Water then drained more gently from the chamber as the air bubble passed through the plug and thus reduced the pressure as the start of the cycle was approached again. Perhaps contrary to expectation, the chugging seemed more severe with the bell-mouth entry.

In an attempt to damp the chugging a 25 mm thick layer of matting was placed 78 mm above the top of the discharge tube, as shown in figure 3. The matting was composed of spun plastic fibre with 97 per cent free volume and gave a more even flow of air through the water above the matting. It will be seen that it modified the results for the square-edged entry but had negligible influence upon the results for the bell-mouth.

Chugging continued to be observed when air was drawn from the top of the water chamber to increase the air flow through the discharge tube but its severity tended to decrease. The airflow was almost steady with the square-edged inlet for the highest air flowrates that could be obtained but some chugging was still apparent for the bell-mouth.

### 3. THEORY

The theory is presented in detail in the appendix and is based upon equations set up for lossless waves by Gardner (1977) but with losses in each phase now included.

It is shown that, in essence, Wallis (1969) defined the condition for a small disturbance to be held stationary to be given by two equations:

$$F_H^2 = \frac{\rho_H v_H^2 A_1^2}{\Delta \rho g H} = A_1^4 \left( \frac{A'}{wH} \right) \quad [1]$$

$$F_L^2 = \frac{\rho_L v_L^2 (1 - A_1)^2}{\Delta \rho g H} = (1 - A_1)^4 \left( \frac{A'}{wH} \right) \quad [2]$$

where subscripts  $H$  and  $L$  designate heavy and light phases,  $\rho$  is density,  $\Delta \rho$  is density difference between the phases,  $v$  is velocity,  $g$  is acceleration due to gravity,  $A_1$  is the fractional area occupied by the heavy phase,  $H$  is the depth of the channel,  $A'$  is the cross-sectional area of the channel and  $w$  is the width of the interface between the phases.

$A_1$  is eliminated between [1] and [2] to obtain an equation relating  $F_H$  and  $F_L$ :

$$F_L^{1/2} + (-F_H)^{1/2} = \left( \frac{A'}{wH} \right)^{1/4} \quad [3]$$

Wallis only derived the form of [3] applicable to closed horizontal rectangular channels:

$$F_L^{1/2} + (-F_H)^{1/2} = 1 \quad [4]$$

and this has been widely used as a guide to the correlation of data for vertical tubes, though not to horizontal systems.

Now, although [1] and [2] define conditions for which a small disturbance is stationary, the Appendix shows that the only necessary condition is that:

$$\frac{F_H^2}{A_1^3} + \frac{F_L^2}{(1 - A_1)^3} = \left( \frac{A'}{wH} \right) \quad [5]$$

It is to be noted that Wallis differentiated [5] with respect to  $h_1$  for a rectangular channel with  $F_L$  and  $F_H$  held constant. He thus retrieved [1] and [2] and formulated [4]. Equations [1]

and [2] are not retrieved if the same process is carried out for a tube and consistency would demand that [5] were solved simultaneously with the differentiated [5]. Systems can be visualized where this process is appropriate.

The extra degree of freedom made available by accepting [5] alone as the condition for stationary small disturbances is exercised to examine the velocity of finite disturbances when [5] obtains. It is suggested that the condition extra to that of [5] to define flooding is that the rate of change of disturbance height with respect to its velocity is zero when the disturbance height is zero. As a result, the flooding condition is defined by the following two equations:

$$F_H = - \left( \frac{A'}{wH} \right) \frac{A_1^2}{[A_1 + P^2(1 - A_1)]^{1/2}} \tag{6}$$

$$F_L = \left( \frac{A'}{wH} \right) \frac{P(1 - A_1)^2}{[A_1 + P^2(1 - A_1)]^{1/2}} \tag{7}$$

instead of by [1] and [2]. Most importantly, the flooding condition now depends upon the ratio of the phase densities in the form:

$$P = \left( \frac{\rho_H}{\rho_L} \right)^{1/2} \tag{8}$$

In the case of a rectangular channel the flooding condition reduces to:

$$F_H = \frac{-h_1^2}{[h_1 + P^2(1 - h_1)]^{1/2}} \tag{9}$$

$$F_L = \frac{P(1 - h_1)^2}{[h_1 + P^2(1 - h_1)]^{1/2}} \tag{10}$$

The relationship between  $F_L$  and  $F_H$  for flooding, with  $P$  as a parameter, is shown in figure 4 for a closed horizontal rectangular channel and in figure 5 for a horizontal pipe. Figure 6 shows the fractional height occupied by the heavy phase versus  $(-F_H)^{1/2}$  for  $P = 29$ , which is the value of the air-water system at atmospheric pressure. Figure 6 gives curves for both rectangular channels and pipes and also gives the predictions based upon [1].

The prediction of flooding is for a system with an unlimited volume of the heavy fluid at one

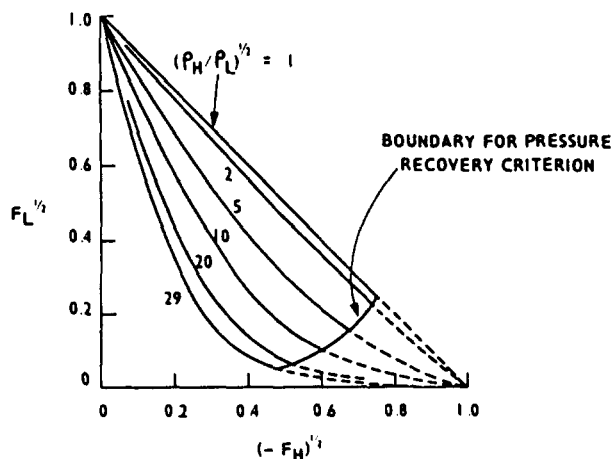


Figure 4. The new flooding criterion for a horizontal channel.

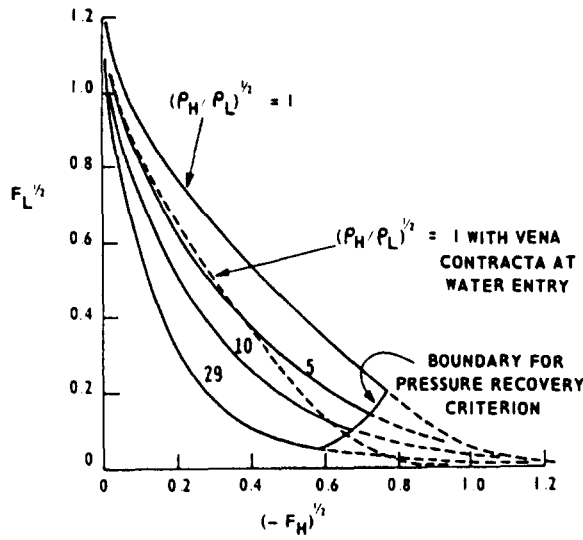


Figure 5. The new flooding criterion for a horizontal pipe.

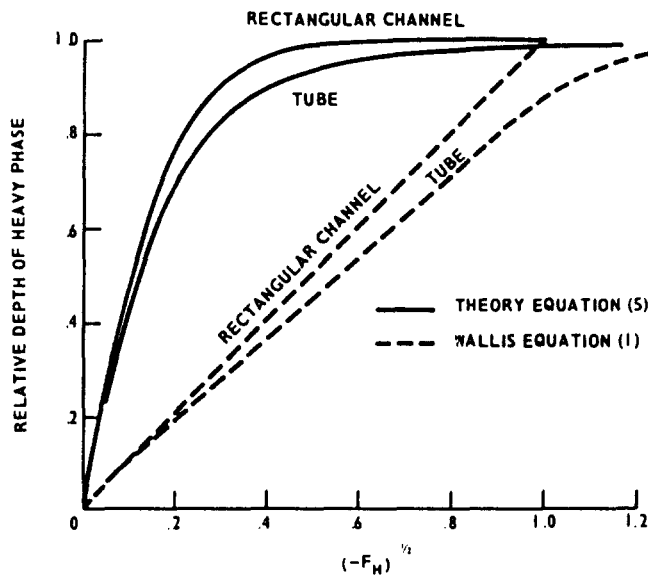


Figure 6. Relative depth of heavy phase at flooding.

end of the channel and an unlimited volume of the light fluid at the other end. The condition with respect to air was met in the experiments described in the last Section and the condition with respect to water was essentially met since the discharge rate of water was found to be unaffected as the level fell in the experimental tank. However, it is to be expected that the water level would become a variable if the level fell too far.

A further restriction on the application of the theory is formulated with reference to figure 3 as follows. Let  $p_0$  be the pressure in the water tank far from the discharge pipe and at the level of the bottom of the pipe. The pressure in the pipe at the same level is therefore  $[p_0 - \frac{1}{2}\rho_H v_H^2]$  and the pressure at the top of the channel is this value less  $H[\rho_H g h_1 + \rho g(1 - h_1)]$ . Now the air pressure cannot rise by more than  $\frac{1}{2}\rho_L v_L^2$  upon discharge and, since the pressure in the tank far from the discharge pipe increases by  $\rho_H g H$  over the depth  $H$ , a necessary condition for the

validity of the theory becomes:

$$\frac{F_L^2}{(1-A_1)^2} \geq \frac{F_H^2}{A_1^2} - 2(1-h_1). \quad [11]$$

The region where the theory is invalid, which is for high values of  $(-F_H)^{1/2}$ , is indicated by dotted lines in figures 4 and 5.

It is interesting to note that the equal volume exchange flow which occurs when pouring a beverage from a bottle occurs in the region where condition [11] is not met. It is possible that this condition denotes the region where chugging is inevitable, though it does not exclude the possibility of chugging outside that region.

#### 4. THE EXPERIMENTAL RESULTS

The experimental results for the square-edged and bell-mouth entries are given in figures 7 and 8 respectively. They mostly lie above the theoretical line but far below the line for  $P = 1$  in figure 5, which is the equivalent of Wallis' (1969) prediction for flooding applied to a tube. No measurements were made of the depth of the air layer but the qualitative observation was that it was small. Its value would certainly not agree with the prediction based upon [1], which is

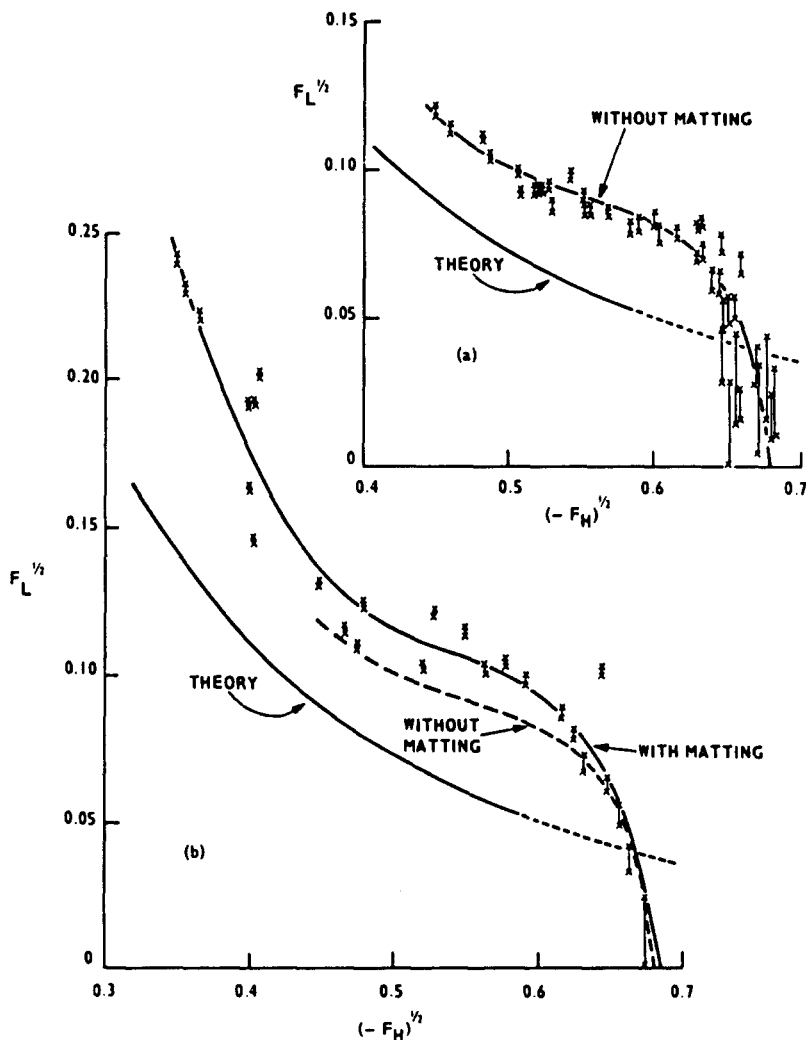


Figure 7. Experimental results for square-edged entry: (a) without matting; (b) with matting.

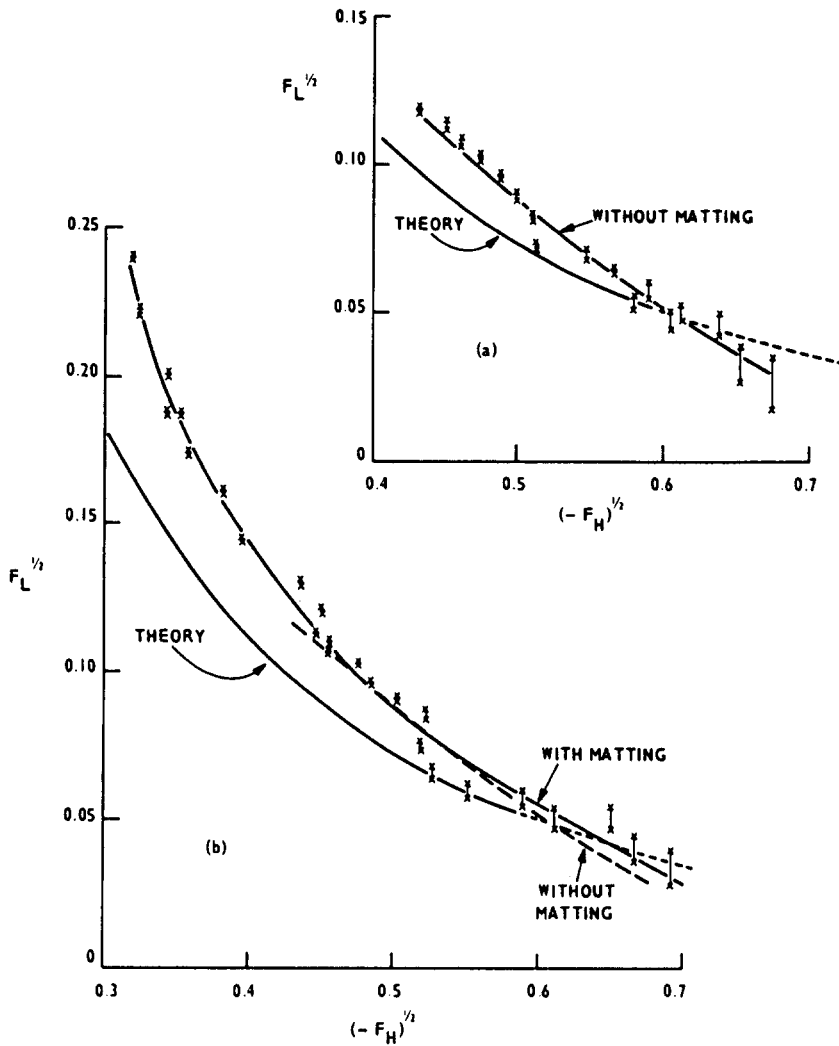


Figure 8. Experimental results for bell-mouth entry: (a) without matting; (b) with matting.

given in figure 6, but would be better represented by the prediction of the present theory, which is also presented in figure 6.

A probable reason for the discrepancy between theory and experiment is the observed erratic nature of the flow. However, it is noted that the results for the bell-mouthed entry are closer to the theoretical line, even though chugging was more pronounced than for the square-edged entry. Also, the matting, which had a slight calming effect, moved the results for the square-edged entry away from the theoretical line, but had no influence on the results for the bell-mouthed entry.

A feature of the results with the square-edged entry is that they start to dip down at  $(-F_H)^{1/2}$  between 0.56 and 0.6 and the maximum value of  $(-F_H)^{1/2}$  is 0.68 when  $F_L = 0$ . This may be associated with inability of the air to recover sufficient pressure upon discharge when  $(-F_H)^{1/2}$  exceeds 0.585. Indeed, chugging was most severe when  $(-F_H)^{1/2}$  exceeded this value and became progressively less severe as  $(-F_H)^{1/2}$  decreased from 0.585. No equivalent dip is seen with the results for the bell-mouthed entry and this may be due to the different manner in which the air was discharged, although chugging was even more severe.

Lastly, it should be noted that the theory is one-dimensional, whereas the convergent flow of water into a tube is strongly three-dimensional. It would be of interest to carry out work with



a rectangular channel to determine if better agreement between theory and experiment is obtained.

#### 5. THE DATA OF RICHTER *et al.* (1978) AND KROLEWSKI (1980)

Richter *et al.* (1978) used the apparatus illustrated in figure 1, which is a third scale model of the relevant features of a PWR hot leg and steam generator inlet plenum. The fluids were air and water at atmospheric pressure and the horizontal hot leg diameter was 203 mm. Water was injected at one of two positions identified as positions 1 and 2 in 1. Their data are plotted in 9 and they all have  $F_L^{1/2}$  greater than 0.5.

Krolewski (1980) used the five systems in figure 2, which are identified by the letters A to E. Air and water at atmospheric pressures were used and the horizontal pipe diameter was 51 mm. Her data are also plotted in 9 and all has  $F_L^{1/2}$  less than 0.5. They are the data that she obtained by slowly reducing the air flowrate while maintaining a water flow into the tank. She also obtained data by raising the air flowrate with a constant water flow and noting when the water started to be held up. Most of these data are represented by points slightly above those in figure 9 but, in the case of systems C and E, in which the pipe slopes down from the water tank at an angle of  $45^\circ$ , these data points were substantially above those in 9 when  $(-F_H)^{1/2}$  exceeded about 0.25. The plotted data points are of interest here because they represent conditions for which the water inlet was well flooded.

Figure 9 contains the theoretical line for  $P = 29$ , which corresponds to the atmospheric air-water system. It also contains smooth lines drawn through the data of the present experiments.

It is seen that there is little difference between the data for Krolewski's systems over most of the data range and her data is mostly in agreement with the results for the different systems of the present work. However, the following exceptions are noted.

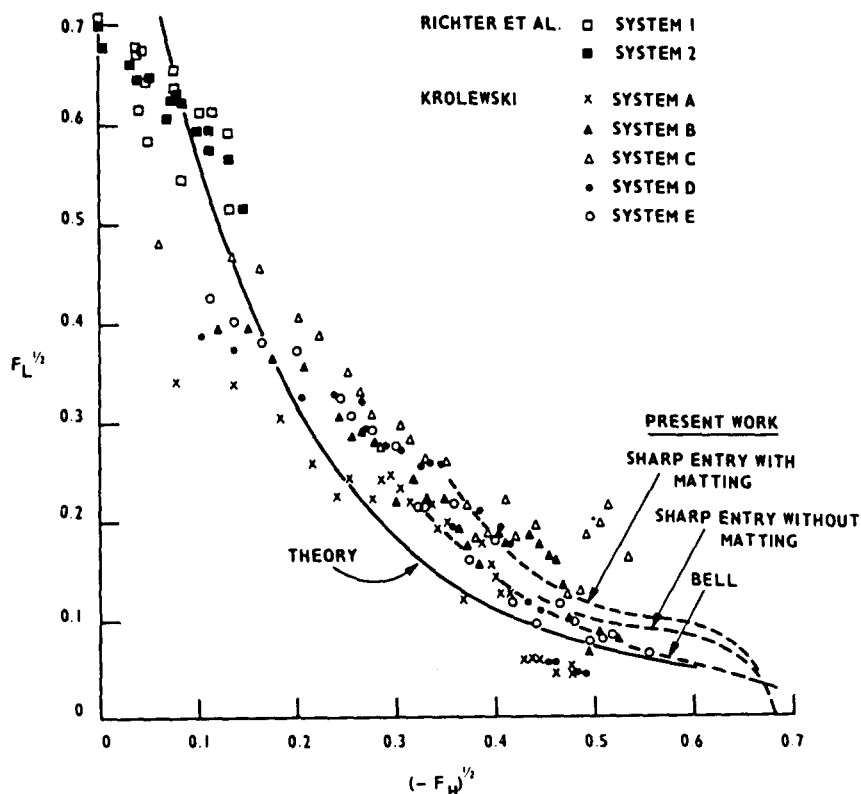


Figure 9. All the data for air and water systems at atmospheric pressure.

A substantial number of data points for systems *A* and *D*, which have vertical pipes leading down from the tank to the horizontal pipe, fall well below the other points and the theoretical line when  $(-F_H)^{1/2}$  is greater than 0.43. There is no obvious reason why this should occur for those systems and not for the remaining system *B*, which has a vertical pipe. The fall occurs for much smaller water flowrates than for the pipe with a sharp entry of the present work but perhaps the cause is similar.

Data points for system *E* tend to be higher than the others for  $(-F_H)^{1/2}$  greater than 0.45. The form of the cut back entry into the sloping pipe may be causing this. It may allow air to escape without interacting strongly with the water inflow. In consequence, water might accelerate more readily down the sloping pipe and the system might be tending to one corresponding to Wallis' flooding criterion, though comparison with figure 6 indicates that it is still a long way from it.

All of Krolewski's systems individually tend to have smooth correlating lines which cross the theoretical line from right to left as  $(-F_H)^{1/2}$  is reduced. If system *A* is ignored because it has the complicating feature of a vertical drain pipe of the same diameter as the horizontal pipe, the crossing takes place at  $(-F_H)^{1/2}$  between 0.14 and 0.18 and extrapolation might indicate that  $(-F_H)^{1/2}$  would become zero at between  $F_L^{1/2}$  between 0.45 and 0.55. This is at variance with the data of Richter *et al.* (1978) whose system 1 bears a close resemblance to system *E* and even to system *C*. Richter's data indicates  $F_L^{1/2} = 0.7$  at  $(-F_H)^{1/2} = 0$  and it crosses the theoretical line at about  $(-F_H)^{1/2} = 0.08$ .

Viewing all of Krolewski's, Richter's and the present data together there is a fair measure of agreement with the theoretical interpretation but the reservations made, especially in the last paragraph, need to be borne in mind. However and notwithstanding the reservations, the closeness of the theoretical line to the experimental points emphasises that the density ratio of the two phases is probably an important parameter besides the Froude numbers  $F_L$  and  $F_H$ .

6. DATA FOR MISCIBLE FLUIDS WITH  $P$  CLOSE TO UNITY

All the data for miscible fluids was for systems in which there was equal volumetric exchange of fluids. Therefore, when  $P = 1$ , the theoretical value of  $F_L^{1/2}$  lies on a line through the origin with a slope of 45° in 6. As  $P$  increases, the value of  $F_L^{1/2}$  decreases not only because the curves in 5 then lie below that for  $P = 1$  but also because the appropriate line through the origin will have a slope of less than 45°.

Theoretical lines of  $F_L^{1/2}$  vs  $P^2$  are drawn in figure 10 for heavy phase inlet flows without a

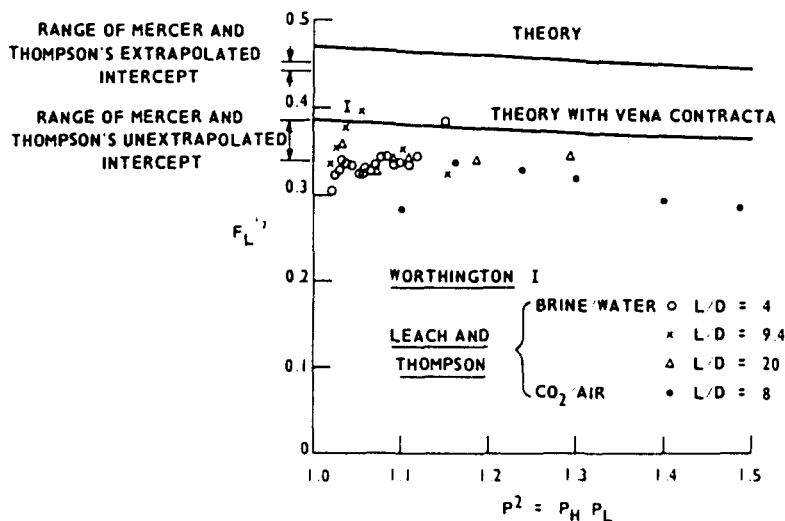


Figure 10. The data for miscible fluids with a small density ratio.

vena contracta and also with a vena contracta, which reduces the heavy phase flow area to 62 percent of that occupied by the heavy phase.

Most of the data are due to Leach & Thompson (1975) and mostly lie below but reasonably close to the theoretical line for a system with a vena contracta. A few points lie closer to this line, as do the limited results of Witherington (1975). Leach and Thompson's results follow the expected trend of  $F_L^{1/2}$  with  $P^2$ .

Mercer & Thompson (1975) carried out experiments in which a tank containing brine and with a discharge tube set normal to one wall of the tank could be tilted in a larger tank of water. The range of their experimental values when the discharge tube was horizontal is indicated in figure 10 and are seen to be in agreement with the other experimental data. However, values obtained by extrapolating Mercer & Thompson's data to conditions for a horizontal tube are also given in figure 10 and they lie close to the theoretical line for a system without a vena contracta. The reason for this is not clear but it is improbable that it might be because tilting the tube suppressed the phenomenon of chugging. It is common experience that over-tilting a bottle of liquid only makes chugging more obvious. In agreement with this, the bell-mouth entry of the present experiments, shown in figure 3, tended to encourage chugging and the bell-mouth might be expected to help in discharging the lighter fluid in the same fashion as the tilting of the discharge tube.

Mercer & Thompson's (1975) graph of results are reproduced in 11 because they indicate that a fairly constant value of discharge is maintained, from an angle to tilt close to zero up to 20–30° to the horizontal, when the length to diameter ratio of the discharge tube is 3.5, so that the extrapolation noted above is not in much doubt. (N. B. Mercer and Thompson may have incorrectly speculated upon the trend of the curve between the point at zero tilt and the point at about 12° tilt.) The reason why curves for larger values of length to diameter ratio fall more rapidly may be that sufficient length may then be available to develop larger interfacial waves which, in the writer's experience, develop for exchange flows in sloping tubes.

## 7. DISCUSSION

The theoretical treatment of lossless waves by Gardner (1977) has allowed an examination of flooding to be made for tubes as well as rectangular channels. It has also been concluded that the ratio of densities of the two fluids employed has an influence beyond that expressed in the previous flooding criteria of Wallis (1969).

Figure 9 shows that, although the flow was unstable over much of the range and exhibited chugging, much of the experimental data lies fairly close to the theoretical prediction. There

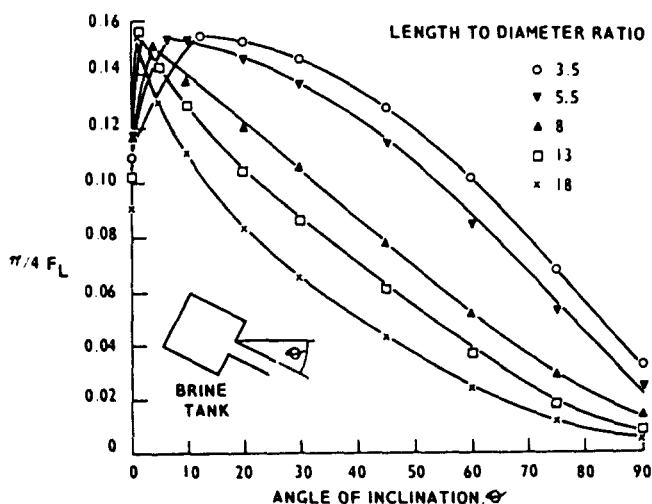


Figure 11. Experimental results of Mercer and Thompson (1975).

appears to be only a small influence of the entry configuration over most of the flow range. The variables included in the theory are those usually assumed to be important in problems associated with pipe entries and it is noted, in particular, that viscosity is usually found to have a negligible effect. There is more doubt, however, that surface tension may not be important because of the narrowness of the gap, through which the air discharges. Also, experience with flooding in vertical tubes shows that surface tension can become important when the size of the system and thus the light phase velocity increases. Drops may then be torn from the heavy phase. However, it must also be noted that the experiments with miscible fluids, where the surface tension is zero, tend to contradict any expectation that entrainment of one fluid by the other is a factor.

Lastly, the conclusions obtained from figure 9, where  $P = 29$ , are not wholly compatible with those of figure 10, where  $P$  is close to unity. The results in figure 9 lie slightly above a theoretical line, which is derived without consideration of a vena contracta. Most of the results of figure 10 lie slightly below a line, which allows for a vena contracta. However, the results in figure 10 were all obtained with a discharge tube about half full of each phase and this is only true in figure 9 for  $(-F_H)^{1/2}$  less than about 0.1, when the experimental points in general lie beneath the theoretical line. Therefore the data of figure 10 is not necessarily incompatible with that of figure 9. This comment reinforces the view that more experimental work is needed, preferably with a rectangular channel.

*Acknowledgements*—The experimental work was carried out by Miss J. A. Finn, who was an engineering undergraduate on vacation from Oxford University. The work was carried out at the Central Electricity Research Laboratories and is published by permission of the Central Electricity Generating Board.

#### REFERENCES

- GARDNER, G. C. 1977 Motion of miscible and immiscible fluids in closed horizontal and vertical ducts. *Int. J. Multiphase Flow* 3, 305–318.
- KROLEWSKI, S. M. 1980 Flooding limits in a simulated nuclear reactor hot leg. Massachusetts Institute of Technology submission as part of requirement for a B.Sc.
- LEACH, S. J. & THOMPSON, H. 1975 An investigation of some aspects of flow into gas-cooled nuclear reactors following an accidental depressurization. *J. Br. Nucl. Energy Soc.* 14, 243–250.
- MERCER, A. & THOMPSON, H. 1975 An experimental investigation into some further aspects of the buoyancy-driven exchange flow between carbon dioxide and air following a depressurization accident in an Magnox reactor. *J. Br. Nucl. Energy Soc.* 14, 327–334.
- RICHTER, H. J., WALLIS, G. B., CARTER, K. H. & MURPHY, S. L. 1978 De-entrainment and countercurrent air–water flow in a model PWR hot leg. NRC-0193-9.
- WALLIS, G. B. 1969 *One-dimensional Two-phase Flow*. McGraw-Hill, New York, Chap. 6.
- WITHERINGTON, D. 1978 Model tests to determine the buoyancy-driven air ingress rate to a depressurized Magnox reactor. Berkeley Nuclear Laboratories, RD/B/N4410.

#### APPENDIX

The analysis of Gardner (1977) for lossless waves in closed horizontal ducts will be followed but terms for losses will now be included.

Figure 12 illustrates the system, subscripts  $L$  and  $H$  designate light and heavy phases and subscripts 1 and 2 designate stations 1 and 2 at which the flow is assumed to be one-dimensional,  $v$  is the true velocity,  $H$  is the depth of the channel,  $A'$  is the cross-sectional area of the channel,  $A'_1$  or  $A'_2$  is the cross-sectional area of the heavy phase and  $h'$  is the depth of the heavy phase. The centre of pressure of the area  $(A'_2 - A'_1)$  is at a distance  $y'$  below the interface at station 2 and  $p$  is the pressure at the interface.  $\rho$  is the density,  $\Delta\rho$  is the pressure difference between the phases and  $e$  is the specific energy loss.

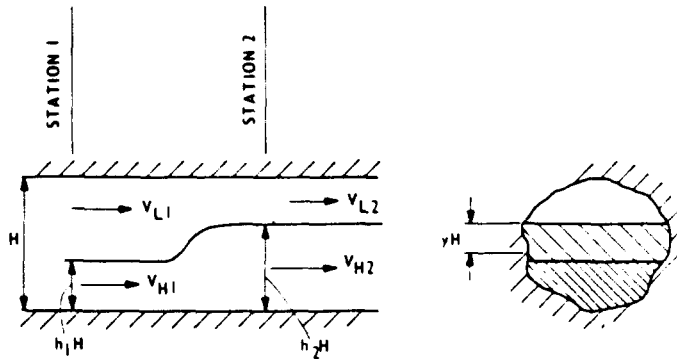


Figure 12. A lossless wave.

Conservation of energy between the two phases is given by:

$$p_1 + \frac{\rho_H v_{1H}^2}{2} + \rho_H g h_1' = p_2 + \frac{\rho_H v_{2H}^2}{2} + \rho_H g h_2' - e_H \quad [A1]$$

$$p_1 + \frac{\rho_L v_{1L}^2}{2} - \rho_L g (H - h_1') = p_2 + \frac{\rho_L v_{2L}^2}{2} - \rho_L g (H - h_2') + e_L \quad [A2]$$

It is noted that both of the energy losses are positive but that the heavy phase is assumed to have a negative velocity.

The dynamic force balance over the whole channel cross-section is:

$$\begin{aligned} & \rho_H v_{1H}^2 A_1' + \rho_L v_{1L}^2 (A' - A_1') + p_1 A' + \rho_H g A_1' x_{1H}' - \rho_L g (A' - A_1') x_{1L}' \\ & = \rho_H v_{2H}^2 A_2' + \rho_L v_{2L}^2 (A' - A_2') + p_2 A' + \rho_H g A_2' x_{2H}' \\ & - \rho_L g (A' - A_2') x_{2L}' \end{aligned} \quad [A3]$$

where  $x'$  is the distance of the centre of pressure of the phase from the interface.

Continuity relations are:

$$A_1' v_{1H} = A_2' v_{2H} \quad [A4]$$

$$(A' - A_1') v_{1L} = (A' - A_2') v_{2L} \quad [A5]$$

Also the following relationships concerning the centres of pressure can be derived by elementary means:

$$A_2' x_{2H}' - A_1' x_{1H}' = (A_2' - A_1') y' + (h_2' - h_1') A_1' \quad [A6]$$

$$(A' - A_2') x_{2L}' - (A' - A_1') x_{1L}' = (A_2' - A_1') y' - (h_2' - h_1') (A' - A_1') \quad [A7]$$

The pressure difference  $(p_2 - p_1)$  is eliminated between [A1] and [A3] and [A4] to [A7] are used to achieve:

$$\frac{F_{1H}^2}{A_1'^2 A_2'^2} \left[ \frac{A_1 + A_2}{2} - A_1 A_2 \right] + \frac{F_{1L}^2}{(1 - A_1)(1 - A_2)} + y \quad [A8]$$

$$- (1 - A_1) \left[ \frac{h_2 - h_1}{A_2 - A_1} \right] + \frac{E_H}{(A_2 - A_1)} = 0 \quad [A8]$$

and a similar process of elimination between [A2] and [A3] yields:

$$\frac{F_{iH}^2}{A_1 A_2} + \frac{F_{iL}^2}{(1-A_1)^2(1-A_2)^2} \left[ \frac{A_1 + A_2}{2} - A_1 A_2 \right] - y - A_1 \left[ \frac{h_2 - h_1}{A_2 - A_1} \right] + \frac{E_L}{(A_2 - A_1)} = 0 \quad [A9]$$

where

$$F_{iH}^2 = \frac{\rho_H v_{iL}^2 A_1^2}{\Delta \rho g H}, \quad F_{iL}^2 = \frac{\rho_L v_{iL}^2 (1-A_1)^2}{\Delta \rho g H} \quad [A10]$$

$$h_1 = \frac{h'_1}{H}, \quad h_2 = \frac{h'_2}{H}, \quad y = \frac{y'}{H} \quad [A11]$$

$$A_1 = \frac{A'_1}{A'}, \quad A_2 = \frac{A'_2}{A'} \quad [A12]$$

$$E = \frac{e}{\Delta \rho g H}. \quad [A13]$$

It is noted that  $F_{iH}$  is the same as Wallis' (1969)  $j_H$  since the fractional area  $A_1$  has been employed to give the superficial velocity ( $v_{iH} A_1$ ).

The subscript 1 will be removed from  $F_{iH}$  and  $F_{iL}$  in the remaining text since the value of this group at station 2 will not be required.

Equations [A8] and [A9] are solved for  $F_H$  and  $F_L$ :

$$\frac{F_H^2}{A_1^2 A_2^2} = \frac{2}{(A_2 - A_1)^2} [(1 - A_1)(h_2 - h_1) - (2 - A_1 - A_2)y] - \frac{4}{(A_2 - A_1)^3} \left[ E_H \left( \frac{A_1 + A_2}{2} - A_1 A_2 \right) - E_L (1 - A_1)(1 - A_2) \right] \quad [A.14]$$

$$\frac{F_L^2}{(1 - A_1)^2 (1 - A_2)^2} = \frac{2}{(A_2 - A_1)^2} [(A_1 + A_2)y - A_1(h_2 - h_1)] + \frac{4}{(A_2 - A_1)^3} \left[ E_H A_1 A_2 - E_L \left( \frac{A_1 + A_2}{2} - A_1 A_2 \right) \right]. \quad [A15]$$

If  $(A_2 - A_1)$  is made vanishingly small, [A14] and [A15] are only meaningful if energy losses reduce to zero. The equations then become:

$$F_H^2 = A_1^4 \frac{A'}{wH} \quad [A16]$$

$$F_L^2 = (1 - A_1)^4 \frac{A'}{wH} \quad [A17]$$

where  $w$  is the width of the interface.

Elimination of  $A_1$  between [A16] and [A17] gives:

$$F_L^{1/2} + (-F_H)^{1/2} = \left( \frac{A'}{wH} \right)^{1/4} \quad [A18]$$

which is the generalized form of Wallis' (1969) flooding criterion. For a rectangular channel [A18] reduces to the particular form given by Wallis:

$$F_L^{1/2} + (-F_H)^{1/2} = 1 \quad [\text{A19}]$$

It is interesting that [A18], which is derived for a horizontal rectangular channel, has only been applied to aid the correlation of data for flooding of vertical tubes.

Now [A18] and [A17] describe values of  $F_H$  and  $F_L$ , for which a small disturbance will remain stationary. However, they are not necessary values. This is demonstrated by returning to the energy and momentum conservation [A1], [A2] and [A3].  $(p_2 - p_1)$  can be eliminated from any pair of these equations and the result can be reduced to an equation applicable to a vanishingly small disturbance. Independent of the pair chosen we find that:

$$\frac{F_H^2}{A_1^3} + \frac{F_L^3}{(1-A_1)^3} = \frac{A'}{wH} \quad [\text{A20}]$$

and it may be checked that the particular choice of  $F_H$  and  $F_L$  given by [A16] and [A17] agrees with [A20] which is the necessary condition for a stationary small disturbance. It follows that condition [A18] for flooding may be incorrect because all the possible combination of  $F_H$  and  $F_L$  for a small disturbance have not been examined.

In order to simplify the algebra, we will now proceed by considering a rectangular channel when [A14] and [A15] become:

$$\frac{F_H^2}{h_1^2 h_2^2} = 1 - \frac{2E_H}{(h_2 - h_1)} + \frac{4E_L(1-h_1)(1-h_2)}{(h_2 - h_1)^3} \quad [\text{A21}]$$

$$\frac{F_L}{(1-h_1)^2(1-h_2)^2} = 1 + \frac{4E_H h_1 h_2}{(h_2 - h_1)^3} - \frac{2E_L}{(h_2 - h_1)} \quad [\text{A22}]$$

Equation [A21] is multiplied by  $h_2$  and [A22] is multiplied by  $(1-h_2)$  and the resultant equations are added to achieve:

$$\frac{F_H^2}{h_1^2 h_2} + \frac{F_L^2}{(1-h_1)^2(1-h_2)} = 1 - \frac{2}{(h_2 - h_1)^3} [E_H h_2 (h_2^2 - 2h_1 + h_1^2) + E_L (1-h_2)(h_2^2 - 2h_2 + h_1^2)]. \quad (\text{A23})$$

Equation [A23] clearly reduces to [A20] applied to a rectangular channel when  $E_H = E_L = 0$  and  $h_1 = h_2$ . Therefore, the properties of a system in which a small disturbance is stationary can be examined for the propagation of finite disturbance in which energy losses may occur.

Let us define a coordinate system in which  $F_H = F_{HO}$  and  $F_L = F_{LO}$  and a small disturbance is stationary. Let a disturbance of height  $(h_2 - h_1)$  have a velocity  $v_w$ . Then [A23] can be employed with:

$$\frac{F_H}{h_1} = \frac{F_{HO}}{h_1} - PV, \quad \frac{F_L}{(1-h_1)} = \frac{F_{LO}}{(1-h_1)} - V \quad [\text{A24}]$$

where

$$V = \left[ \frac{\rho_L}{\Delta \rho g H} \right]^{1/2} v_w \quad [\text{A25}]$$

$$P = \left( \frac{\rho_H}{\rho_L} \right)^{1/2}. \quad [\text{A26}]$$

Equations [A24] are substituted in [A23] and the result is expanded to yield:

$$BV^2 + CV + D = 0 \quad [A27]$$

where

$$B = h_2 + P^2(1 - h_2) \quad [A28]$$

$$C = -2 \left[ \frac{h_2}{(1 - h_1)} F_{LO} + \frac{P(1 - h_2)}{h_1} F_{HO} \right] \quad [A29]$$

$$D = \frac{h_2}{(1 - h_1)^2} F_{LO}^2 + \frac{(1 - h_2)}{h_1^2} F_{HO}^2 - h_2(1 - h_2)G \quad [A30]$$

where  $G$  equals the right hand side of [A23].

When  $h_2 = h_1$ ,  $V = 0$ , as already specified, so that  $D = 0$ . Since  $E_H = E_L = 0$  as well under these conditions:

$$\frac{F_{HO}^2}{h_1^3} + \frac{F_{LO}^3}{(1 - h_1)^3} = 1 \quad [A31]$$

and so the basic criterion for a stationary small disturbance is retrieved.

It is further postulated that the most stable condition is that when:

$$\frac{dh_2}{dV} = 0 \quad [A32]$$

obtains. Indeed, this is the only condition which will give a simple answer because when differentiating  $D$  and setting  $h_2 = h_1$  terms are obtained involving  $(dE/dh_2)$   $(dh_2/dV)$ , which need to equal zero if the energy dissipation is to be ignored. Applying the criterion we find that  $C = 0$  or:

$$\frac{F_{LO}}{(1 - h_1)^2} + \frac{PF_{HO}}{h_1^2} = 0 \quad [A33]$$

Simultaneous solution of [A31] and [A33] gives:

$$F_{LO} = \frac{P(1 - h_1)^2}{[h_1 + P^2(1 - h_1)]^{1/2}} \quad [A34]$$

$$F_{HO} = \frac{-h_1^2}{[h_1 + P^2(1 - h_1)]^{1/2}} \quad [A35]$$

Equations [A34] and [A35] define the values of  $F_{LO}$  and  $F_{HO}$  for the flooding condition for a closed rectangular channel with  $h_1$  as a parameter.

The same analysis can be carried out for a closed channel of arbitrary cross-sectional shape with the result that:

$$F_{LO} = \frac{A^{1/2}P(1 - A_1)^2}{(wH)^{1/2}[A_1 + P^2(1 - A_1)]^{1/2}} \quad [A36]$$

$$F_{HO} = \frac{-A^{1/2}A_1^2}{(wH)^{1/2}[A_1 + P^2(1 - A_1)]^{1/2}} \quad [A37]$$